621.317.382.029.6

Monograph No. 23
MEASUREMENTS SECTION

ABSOLUTE POWER MEASUREMENT AT MICROWAVE FREQUENCIES

By A. L. CULLEN, Ph.D., B.Sc.(Eng.), Associate Member.

(*The paper was first received 13th June, and in revised form 9th November*, 1951. *It was published as an* INSTITUTION MONOGRAPH *15th February*, 1952.)

SUMMARY

The radiation pressure of electromagnetic waves on a reflecting surface may be used as the basis of a method of power measurement at microwave frequencies. The method is absolute, depending only on measurements of mass, length and time; no secondary electrical standards are involved in the experimental procedure. Moreover, no appreciable power is absorbed by the apparatus.

This method has been compared with a balanced calorimeter wattmeter, and agreement to within 1–2 watts has been obtained in the range 10–50 watts. The major difficulty encountered in obtaining greater accuracy with the radiation-pressure apparatus described is the disturbing effect of convection currents of air, caused by the heating of the reflector by the small fraction of the incident microwave power which is not reflected.

LIST OF PRINCIPAL SYMBOLS

a, b = Dimensions of rectangular waveguide.
A = Normalized characteristic admittance.
B = Normalized susceptance.
c = Velocity of light *in vacuo*.
F = Force due to radiation pressure.
h = Height of ripple.
H = Magnetic field strength.
H_{rms} = R.M.S. magnetic field in incident wave.
I = Moment of inertia.
m, α = Coupling coefficients.
p = Instantaneous value of radiation pressure.
P^{+} = Incident power.
r = Radial co-ordinate.
r_1 = Radius of a circular guide.
r_2 = Ratio of amplitudes in successive swings.
Z_0 = Characteristic wave impedance.
β = Phase constant.
δ = Damping coefficient.
Δ = Penetration depth.
κ_0 = Free-space permittivity.
λ_g = Guide wavelength.
θ = Angular position of movement.
ρ = Field reflection coefficient.
ρ_p = Power reflection coefficient.
χ = Radial propagation coefficient.
μ_0 = Free-space permeability.
ω = Angular frequency.

(1) BASIC PRINCIPLES

(1.1) Introduction

In 1873, Maxwell[1] showed from his electromagnetic theory of light that a beam of radiation falling normally on to a flat surface would give rise to a pressure equal in magnitude to the electromagnetic energy density at the surface. He suggested the possibility of experimental verification in the following words:

> "Such rays falling on a thin metallic disc, delicately suspended in a vacuum, might perhaps produce an observable mechanical effect."

In 1876, Bartoli[2] derived Maxwell's result from the second law of thermodynamics in a very general way, showing that it was applicable to all streams of energy. He also attempted to verify the result experimentally, but was unable to overcome disturbing effects due to the heating of the reflector, which gives rise to convection currents of air and to the radiometer effect, collectively described as "gas action."

Lebedew,[3] using light waves, succeeded in 1900 in eliminating these unwanted effects from the final result, and he was the first to give a reliable demonstration of the reality of radiation pressure. By 1902, Nichols and Hull[4] had made a thorough investigation of the "gas action," and had established the quantitative accuracy of Maxwell's result.

Recently, Carrara and Lombardini[7] have demonstrated the existence of radiation pressure at microwave frequencies, but apart from an indication that the pressure was of the correct order of magnitude, no quantitative results were obtained.

Independently of this work, a quantitative method of measuring power at microwave frequencies by making use of the radiation pressure effect has been put forward.[8] Preliminary experimental results have already been reported;[9] it is the purpose of the present paper to describe the techniques adopted and to explain their theoretical basis.

(1.2) Elementary Theory

Maxwell's derivation of an expression for the pressure of electromagnetic radiation was based upon energy considerations and gave no indication of the mechanism of the effect. Sir J. J. Thomson later obtained the same result by considering the mechanical force exerted by the magnetic field of the wave on the currents induced by it in the reflecting surface.

This more physical approach will be followed here to prove the desired result. Consider a simple harmonic plane wave normally incident on a highly conducting surface. The wave will be almost completely reflected at the surface with approximate doubling of the magnetic field and partial cancellation of the electric field. Some energy will flow into the conductor, but will penetrate only slightly, in accordance with the well-known skin-effect. Inside the conductor, displacement current will be swamped by conduction current; if the instantaneous magnetic field in the conductor is H, and the instantaneous current density is ι, curl $H = \iota$ at all points.

With a Cartesian co-ordinate system, and OX as the direction of propagation of the plane wave, OY as the direction of the electric vector, and OZ as the direction of the magnetic vector, and the conductor surface perpendicular to the OX axis, this reduces to

$$\partial H_z/\partial x = -\iota_y \quad . \quad . \quad . \quad . \quad . \quad . \quad . \quad (1)$$

Consider a volume element $dxdydz$ inside the conductor. The current passing through this element is $\iota_y dxdydz$, and its length in the direction of the current is dy. Thus the force on the element (Bli) is $B_z\iota_y dxdydz$ or $\mu_0 H_z\iota_y dxdz$. This may be regarded as a pressure acting on the side $dydz$ and equal to $\mu_0 H_z\iota_y dx$.

The total instantaneous pressure, p, is found by integrating the

Dr. Cullen is at University College, London.

The paper is based on part of a thesis approved for the degree of Doctor of Philosophy in the University of London.

Written contributions on Monographs are invited for consideration with a view to publication.

pressures on the sides of all such elements; thus, if the conductor is semi-infinite

$$p = \mu_0 \int_0^\infty H_z i_y dx$$

Using eqn. (1)

$$p = -\mu_0 \int_0^\infty H_z dH_z$$

$$= \left[-\tfrac{1}{2}\mu_0 H_z^2 \right]_0^\infty$$

and since $H_\infty = 0$

$$p = \tfrac{1}{2}\mu_0 H_{z0}^2 \quad . \quad . \quad . \quad . \quad . \quad . \quad . \quad (2)$$

This equation gives the instantaneous pressure in terms of the instantaneous magnetic field at the conductor surface.

It is more useful in practice to know the average pressure over a long period of time, so that if H_{rms} is the r.m.s. value of the magnetic field, the average pressure $\bar{p}$ is

$$\bar{p} = \tfrac{1}{2}\mu_0 H_{rms}^2 \quad . \quad . \quad . \quad . \quad . \quad . \quad . \quad (3)$$

The total force F exerted on reflecting surface by a beam of cross-sectional area a' is given by

$$F = \tfrac{1}{2}\mu_0 H_{rms}^2 a' \quad . \quad . \quad . \quad . \quad . \quad (4)$$

The experimental verification of this equation presents some difficulty, because H_{rms} cannot be measured directly. In the experiments of Nichols and Hull, the following procedure was adopted:

(*a*) First, the pressure of a given beam of radiation on a reflecting surface was determined.

(*b*) Secondly, the beam of radiation was allowed to fall on a wholly absorbing surface, and the resulting temperature rise was employed to calculate the incident power $P+$ in the beam.

(*c*) Finally, the power-reflection coefficient ρ_p of the reflecting surface was determined.

The details of experimental technique are not relevant at present, but it is necessary to consider the calculation of H_{rms} from p and ρ_p. If displacement currents in the conductor are neglected, the reflection coefficient ρ for the magnetic field can be written as

$$\rho = \left(\sqrt{\frac{\mu_0}{\kappa_0}} - \sqrt{\frac{j\omega\mu_0}{\sigma}}\right) \Big/ \left(\sqrt{\frac{\mu_0}{\kappa_0}} + \sqrt{\frac{j\omega\mu_0}{\sigma}}\right)$$

$$= \left(1 - \sqrt{\frac{j\omega\kappa_0}{\sigma}}\right) \Big/ \left(1 + \sqrt{\frac{j\omega\kappa_0}{\sigma}}\right) \quad . \quad (5)$$

This expression can be put into a more convenient form by introducing the free-space wavelength λ and the penetration depth in the metal, Δ.

Since $2\pi/\lambda = \omega\sqrt{(\mu_0\kappa_0)}$ and $\Delta = \sqrt{(2/\omega\mu_0\sigma)}$ it follows that

$$\frac{2\pi\Delta}{\lambda} = \sqrt{\frac{2\omega\kappa_0}{\sigma}}$$

The previous neglect of displacement currents in the metal is now seen to correspond to neglecting $(\Delta/\lambda)^2$ in comparison with unity. It is therefore appropriate to work to the first order in Δ/λ in the following calculation, when eqn. (5) becomes

$$\rho \simeq 1 - (1 + j)2\pi\Delta/\lambda$$

This is the field reflection coefficient; the power reflection coefficient ρ_p is equal to $|\rho|^2$, and so

$$\rho_p \simeq 1 - 4\pi\Delta/\lambda \quad . \quad . \quad . \quad . \quad . \quad (6)$$

If the incident r.m.s. magnetic field strength is H_{rms}^+ and the total r.m.s. magnetic field strength at the surface of the conductor is H_{rms}, then

$$H_{rms}^2 = (H_{rms}^+)^2|1 + \rho|^2$$

$$\simeq 4(H_{rms}^+)^2\left(1 - \frac{2\pi\Delta}{\lambda}\right)$$

Therefore $$H_{rms}^2 \simeq 4(H_{rms}^+)^2\left(\frac{1 + \rho_p}{2}\right) \quad . \quad . \quad . \quad . \quad (7)$$

The incident power in the beam is

$$P+ = \sqrt{\frac{\mu_0}{\kappa_0}}(H_{rms}^+)^2 a' \quad . \quad . \quad . \quad . \quad . \quad (8)$$

Substituting from eqns. (7) and (8) in eqn. (4), and remembering that $c = 1/\sqrt{(\mu_0\kappa_0)}$ where c is the velocity of light

$$F = \frac{P+}{c}(1 + \rho_p) \quad . \quad . \quad . \quad . \quad . \quad (9)$$

This is the equation derived by Maxwell and verified by Nichols and Hull. If the reflector were perfect, ρ_p would be unity. Thus, the upper limit for the force is

$$F = 2P+/c \quad . \quad . \quad . \quad . \quad . \quad (9a)$$

At optical wavelengths, ρ_p will be appreciably less than unity; e.g. for one of the silver reflectors used by Nichols and Hull the value of ρ_p was 0·92. At microwave frequencies, however, almost complete reflection is easily obtained; e.g. in copper, the penetration depth is $1{\cdot}1 \times 10^{-4}$ cm at a wavelength of 10 cm, so that, using eqn. (6), the reflection coefficient differs from unity by about 1 part in 10^4.

The order of magnitude involved is such that, for an incident power of 1 watt, the force is $0{\cdot}677 \times 10^{-8}$ newton or $0{\cdot}667 \times 10^{-3}$ dyne. Clearly, a sensitive apparatus is necessary to detect such a force, and one must expect to find experimental difficulties in its accurate determination.

It is instructive to derive eqn. (9) from a simple quantal treatment in which the beam of radiation is treated as a stream of photons. Let there be n photons per unit volume in the incident beam. Each photon has energy $h\nu$ and momentum $h\nu/c$ and travels with velocity c. The power $P+$ in the incident beam is then

$$P+ = nh\nu ca' \quad . \quad . \quad . \quad . \quad . \quad . \quad (10)$$

If the power-reflection coefficient of the reflector is ρ_p, a fraction ρ_p of the incident photons will be reflected* and a fraction $(1 - \rho_p)$ will be absorbed. Equating force and rate of change of momentum gives

$$F = 2nh\nu a'\rho_p + nh\nu a'(1 - \rho_p)$$

or $$F = nh\nu a'(1 + \rho_p) \quad . \quad . \quad . \quad . \quad . \quad (11)$$

Substitution from eqn. (10) yields

$$F = \frac{P+}{c}(1 + \rho_p)$$

which is in agreement with eqn. (9).

(1.3) Previous Experimental Investigations

The experiments of Lebedew and of Nichols and Hull were similar in principle. The light beam whose radiation pressure is to be measured, falls on a highly reflecting mirror mounted at one end of the torsion arm of a torsion balance, a similar mirror

* It is reasonable to assume that the frequency is unchanged on reflection; phenomena such as fluorescence are therefore excluded.

at the other end of the arm serving as a counterweight. The torsion balance is mounted in a vacuum so that gas action may be minimized, the angular position of the torsion arm being indicated by a lamp, mirror and scale in the usual way. In principle, the scale readings with and without the light source are observed, and from these readings the angle of twist of the suspension may be found. Hence, if the specific couple is known, the torque can be calculated, and since the radius of action of the torsion system is known, the radiation force may be determined.

The radiation pressure due to radio waves was observed in 1930 by Mlle Husson.[5] Radiation of about 17·5 cm wavelength was directed towards a half-wave resonant dipole of aluminium foil, and the pressure of the incident radiation was detected, a quartz-fibre suspension system being used.

Some rather more detailed work was described by Fritz[6] in 1931; the general arrangements were similar to those of Mlle Husson, and forces of the expected order of magnitude were observed.

Carrara and Lombardini[7] were the first to make use of wartime developments in microwave technique to demonstrate radiation pressure. In their experiments, an aluminium reflecting blade was supported at one end of a torsion arm and enclosed in a glass cover. Radiation at a wavelength of 3 cm was directed on this blade and a deflection of the right order of magnitude was observed.

The methods employed by Husson, Fritz, and Carrara and Lombardini are free-wave methods and cannot give accurate quantitative results, because, as the latter point out, an exact calculation of the force for a given power flow involves the solution of an exceedingly difficult diffraction problem.

This difficulty, which was absent from the experiments of Nichols and Hull, arises because the relatively long wavelength prevents the formation of a narrow parallel beam of radiation such as that employed by them. Moreover, since the net power output of the source is eventually radiated into the laboratory, the resulting spatial standing-wave pattern will cause the observer's position to influence the results to some extent.

(2) AN ABSOLUTE METHOD OF POWER MEASUREMENT BY RADIATION PRESSURE

(2.1) Use of Guided Waves

The diffraction and radiation difficulties of Carrara and Lombardini's work may be overcome by using a waveguide to direct the radiation on to the reflector and prevent its subsequent radiation. Consider therefore the force on a reflecting plate closing one end of a wave guide of unspecified cross-section, fed by a perfectly matched source. Let the r.m.s. values of the transverse components of the electric and of the magnetic field strengths in the incident wave be $\mathscr{E}^+$ and H^+ respectively. If the guide is terminated by a matched load, there will be no reflection of the incident wave, and the power supplied to the load can be obtained by integrating the time-average Poynting vector over the cross-section. It is convenient to introduce the wave impedance Z_0 of the waveguide, which, for any air-filled guide supporting an H mode* has the value

$$Z_0 = \frac{\lambda_g}{\lambda}\sqrt{\frac{\mu_0}{\kappa_0}} \quad . \quad . \quad . \quad . \quad . \quad . \quad (12)$$

The power flow then becomes

$$P^+ = \sqrt{\left(\frac{\mu_0}{\kappa_0}\right)}\frac{\lambda_g}{\lambda}\int_S (H^+)^2 dS \quad . \quad . \quad . \quad . \quad (13)$$

where dS is an element of the surface of the cross-section.

* It will be sufficient to restrict our attention to H modes

Next suppose that, with the same matched source supplying an incident wave of the same amplitude as before, the guide is closed by a perfectly reflecting plate. The tangential electric field will be zero at the plate and the transverse component of the magnetic field will be doubled, having the r.m.s. value $2H^+$. The force exerted on the element dS by this field is $\frac{1}{2}\mu_0(2H^+)^2 dS$ so that the total force on the plate is

$$F = 2\mu_0\int_S (H^+)^2 dS \quad . \quad . \quad . \quad . \quad . \quad . \quad (14)$$

Substituting from eqn. (13) gives

$$F = \frac{2P^+}{c}\frac{\lambda}{\lambda_g} \quad . \quad . \quad . \quad . \quad . \quad . \quad . \quad (15)$$

since $\sqrt{(\mu_0\kappa_0)} = 1/c$. This equation is also valid for any E mode, but the proof is omitted. In principle, a method for measuring the output of a microwave oscillator thus exists. If the oscillator is matched to a waveguide closed by a perfectly reflecting piston, the power P^+ which the transmitter would deliver to a matched load terminating the waveguide can be found by measuring the force F on the piston and employing eqn. (15).

The objection to this method in practice is that microwave oscillators depend somewhat critically on the load impedance into which they are coupled. A purely reactive load might result in damage to the oscillator or might even prevent its operation entirely.

It is clear that, if a radiation-pressure system is to be employed, some method must be devised which permits the oscillator to work into a matched load. A method of achieving this result is discussed in the following Section.

(2.2) The T-Junction

It is now well known[10] that a symmetrical waveguide T-junction has many properties in common with a transmission-line T-junction. In particular, a suitably placed piston in the side guide will allow transmission without reflection in the main guide. This property at once suggests a solution to the problem raised at the end of Section (2.1), i.e. to measure the radiation pressure on such a piston, allowing the power to flow on without reflection in the main guide. In these circumstances, the transmitter can work into a perfectly matched load and will be operating under optimum conditions. If the T-junction is compensated so that it behaves exactly like a transmission-line T-junction, it is not difficult to show that the force F_2 acting on a piston in the side arm is given by

$$F_2 = \frac{P_1}{2c}\frac{\lambda}{\lambda_{g2}} \quad . \quad . \quad . \quad . \quad . \quad . \quad . \quad (16)$$

The force is reduced to one-quarter of that given by eqn. (15) because the incident field of the progressive wave* in the main guide is now being sampled without causing reflection; no longer is there the previous doubling of the magnetic field by reflection and resulting quadrupling of the force.

From a practical point of view, it is desirable to use for the side arm of the T-junction a guide of circular cross-section carrying the H_{01} mode. This mode has no radial current flow, so that moving pistons present no difficulty. For the main guide, however, a rectangular guide carrying the H_{01} mode is desirable. Although it would be possible to make a compensated T-junction of this kind, it is not necessary, for it is easy to make use of the known general theory of T-junctions to find the required force/power relationship for an uncompensated T-junction. This theory, given by Allanson, Cooper and Cowling,[11] leads to

* Since the wave in the main guide is progressive, we may write P_1 for P^+.

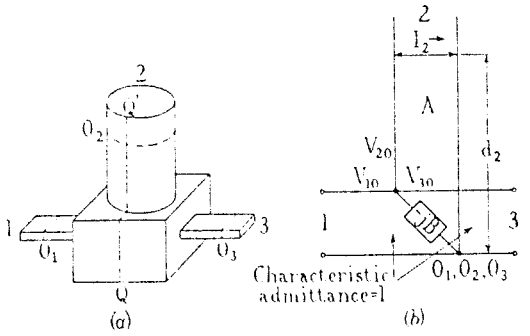

Fig. 1.—Uncompensated symmetrical waveguide T-junction and its equivalent transmission-line junction.

$$A = \frac{\text{Characteristic admittance of leg 2}}{\text{Characteristic admittance of leg 1}}$$

the result that a wave guide T-junction, having symmetry about the plane QQ′ (see Fig. 1), is exactly analogous to a symmetrical shunt transmission-line T-junction with a susceptance at the junction. It is obvious that a correct choice of the short-circuit position on line 2 will cancel the susceptance and allow transmission without reflection. When a short-circuiting piston is placed in the corresponding position in the side arm of the guide junction, transmission without reflection from leg 1 to leg 3 is achieved.

The correct position is found by making use of the formula[11] for the normalized input admittance at a characteristic point O_1 in leg 1 when leg 3 is matched and leg 2 closed by a piston d_2 from a characteristic point* O_2 in leg 2; this may be derived from Allanson, Cooper and Cowling as

$$Y_1 = 1 - j[A \cot \beta_2 d_2 + B] \quad . \quad . \quad . \quad (17)$$

where A is the characteristic impedance of leg 2 normalized to leg 1 [see Fig. 1(*b*)].

The force on a piston at the matching position (where $A \cot \beta_2 d_2 + B = 0$) can easily be shown to be

$$F_2 = \frac{P_1}{2c} \frac{\lambda}{\lambda_{g2}} \left[A + \frac{B^2}{A} \right] \quad . \quad . \quad . \quad . \quad . \quad (18)$$

The form of T-junction used in practice is shown in Fig. 2. The use of slot coupling suggests the application of Watson's theory of slot-coupled T-junctions[12] which, although less general than the preceding theory, has the advantage that it contains a parameter α which depends on slot length, and a parameter m which does not, so that the effect of this variable may be more readily assessed. Watson's m and α are related to A and B by the expressions

$$\left.\begin{aligned} A &= \frac{m}{\alpha^2 + m^2} \\ B &= -\frac{\alpha}{\alpha^2 + m^2} \end{aligned}\right\} \quad . \quad . \quad . \quad . \quad . \quad (19)$$

Substituting in eqn. (19), it follows that

$$F_2 = \frac{P_1}{2c} \frac{\lambda}{\lambda_{g2}} \frac{1}{m} \quad . \quad . \quad . \quad . \quad . \quad (20)$$

This expression is independent of α, so that the force is independent of slot length. This rather surprising result is true only approximately for guide walls of finite thickness, but is fairly accurate for slots about $\lambda/2$ in length, i.e. much longer than the wall thickness.

The values of A and B (or m and α) determine the impedance-transforming properties of the junction, and can be found by measurements of the positions of nodes of the electric field in one guide when the other two are terminated in perfectly reflecting movable pistons. It should be noted that standing-wave-ratio measurements need not be made, so that the detector law is of no consequence. Thus, the relationship between force and power for any T-junction can be found from measurements of length and a knowledge of the velocity of light.

In some simple cases, the constant relating force and power can be calculated theoretically, and such a calculation has been made for the T-junction of Fig. 2.

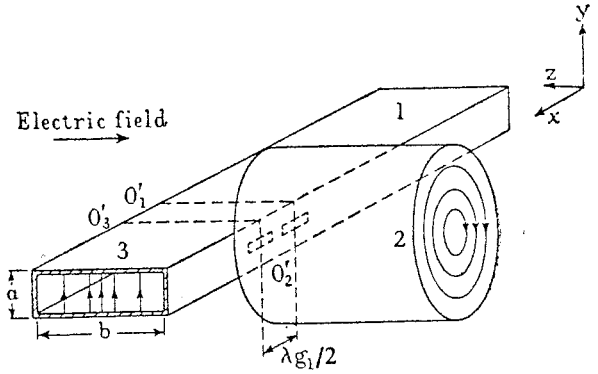

Fig. 2.—Slot-coupled T-junction.

The calculation depends on the result that the current flow in the side wall of the main guide runs through the slot into the side guide without discontinuity when the piston in the side guide is correctly located (see Fig. 3). Thus, since the distributions of

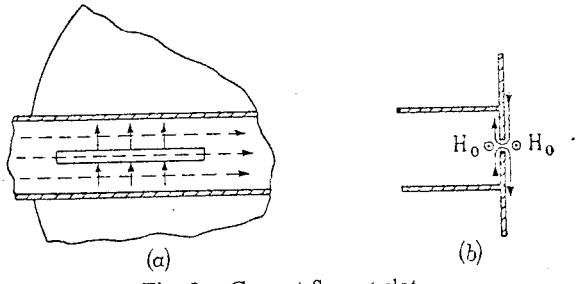

Fig. 3.—Current flow at slot.
(*a*) Current and magnetic field in rectangular guide.
(*b*) Continuity of current at slot.
——→ Current flow.
- - - →- Magnetic field.

radial magnetic field in the circular guide and longitudinal magnetic field in the main guide are very similar, it is reasonable to equate the maximum values of these fields (see Fig. 4).

The details of the calculation will not be given here, but the result is

$$\frac{1}{m} = \frac{\pi r_1^2 \lambda_{g1} \lambda_{g2}}{2ab^3} \left[\frac{J_0(\chi r_1)}{J_1(\chi r)} \right]^2 \quad . \quad . \quad . \quad . \quad (21)$$

where λ_{g1} and λ_{g2} are the guide wavelengths in the main and side guides respectively, r_1 is the radius of the side guide, $\chi r_1 = 3{\cdot}8317$, i.e. the lowest root of the equation $J_1(\chi r_1) = 0$ and $J_1(\chi r)$ is the first maximum of the first-order Bessel function.

(2.3) Experimental Investigation of Mode Purity in Circular Guide

The whole of the preceding theory has been based on the assumption that it is possible to couple the main rectangular and

* A characteristic point, e.g. O_2, in leg 2 is one at which a short-circuiting piston will block transmission from leg 1 to leg 3. The nodes of the resulting standing-wave pattern in leg 1 define the characteristic points, e.g. O_1, in leg 1. The characteristic points, e.g. O_3, in leg 3 follow, in this case, by symmetry.

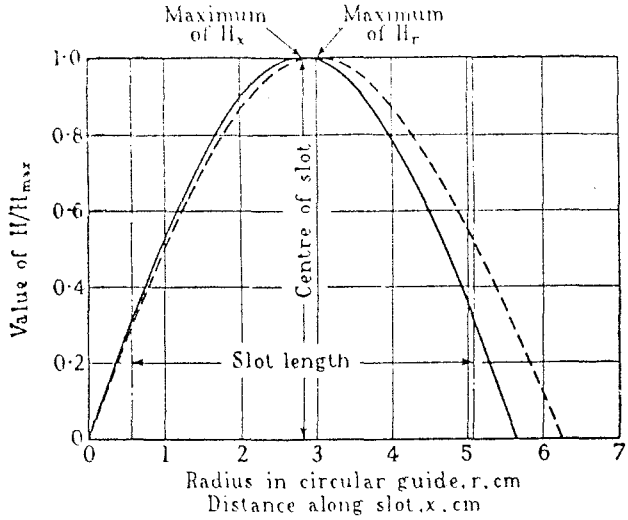

Fig. 4.—Magnetic field strengths in rectangular and cylindrical guides.
——— H_x
- - - - - - H_r

subsidiary circular waveguides in a T-junction in such a way that only one mode is excited in each. The rectangular guide dimensions are so chosen that only the dominant H_{01} mode is propagated, and that all the evanescent modes are rapidly attenuated. However, a circular guide of diameter large enough to support the H_{01} mode will also necessarily support several other modes, and the amplitudes of these unwanted modes must be reduced sufficiently to be negligible. In Table 1, the lower-

Table 1

Critical diameter, cm	5·34	6·95	8·84	11·1	12·2	14·9	15·4
Mode	H_{11}	E_{01}	H_{21}	E_{11} / H_{01}	H_{31}	E_{21}	H_{41}
Critical diameter, cm	15·5	16·0	18·5	18·6	19·5	20·4	
Mode	H_{12}	E_{02}	E_{31}	H_{51}	H_{22}	E_{12} / H_{02}	

order waveguide modes are listed in order of their appearance as non-evanescent modes as the diameter of the guide is increased, together with the critical diameter at which they appear when the free-space transverse electromagnetic wavelength is 9·1 cm.

The diameter of the circular guide employed in the experiments is 12·5 cm; this does not represent an optimum choice, but is the internal diameter of some resonant-cavity "echo boxes" that happened to be available. It will be seen that six propagating modes are possible, namely the E_{01} and E_{11}, and the H_{01}, H_{11}, H_{21} and H_{31} modes. Of these, the E_{01} mode is not excited because it has no radial component of magnetic field, and the modes with odd symmetry, E_{11}, H_{11} and H_{31}, are—ideally—not excited, because the anti-phase slot excitation couples only with those modes having even angular symmetry, namely H_{01} and H_{21}. Departure from the ideal is to be expected, and a certain amount of odd-mode excitation may be anticipated, but the most serious difficulty is clearly the H_{21} mode.

Experiments were therefore made to find the angular distribution of the radial component of the magnetic field in the circular guide of a slot-coupled T-junction. The apparatus used in these experiments is shown in Fig. 5.

Accurate and independent adjustments of the angular and axial positions of the reflecting disc could readily be made.

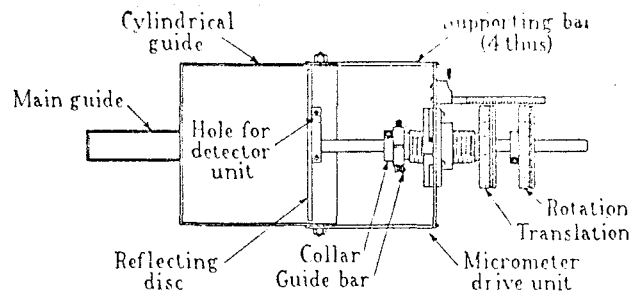

Fig. 5.—Apparatus for T-junction experiments.

Provision of a small hole in the reflecting disc allowed the insertion of the coupling loop of a crystal detector unit, oriented to couple only with the radial magnetic field.

A CV67 klystron operating at 9·10 cm fed into one end of the main guide, the other end being terminated by a well-matched load; preliminary measurements of the angular variation of the radial magnetic field showed considerable variation with rotation, as was expected. An attempt to reduce the H_{11} and H_{21} modes by using wire mode-filters was made, and some improvement was found.

It was then observed that the angular distribution of field and excitation of unwanted modes depended in a marked manner on the axial position of the reflecting disc in the circular guide. For a micrometer-drive setting of 1·77 cm the angular distribution was very nearly uniform, which indicated almost pure H_{01} mode. Standing-wave-indicator measurements showed that this setting closely corresponded with optimum matching in leg 1.

Quite small departures from this setting led to appreciable cyclical variations, and these could be analysed into H_{11} and H_{21} components, as shown in Fig. 6, in which the ordinate represents

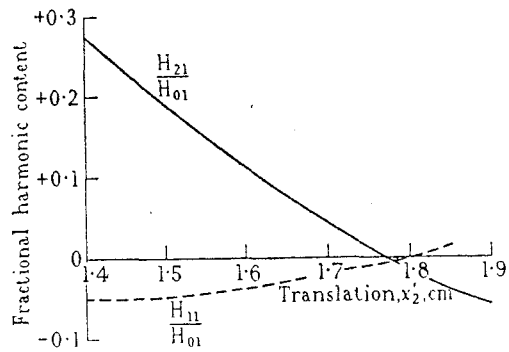

Fig. 6.—Spatial harmonic content of angular field distribution.

the ratio of the radial magnetic field of the unwanted mode to that of the H_{01} mode at a radius of 1·91 cm. The H_{11} mode is always much weaker than the H_{21} mode, and is never more than 5% of the H_{01} field over the range of settings covered. To get a first-order theory of the variation of the angular field pattern with axial disc position x_2 we may therefore neglect the H_{11} mode and consider the variation of the H_{21} mode with x_2. A transmission-line analogue of a waveguide carrying a single propagating mode has already been used, and an extension of this idea leads to the representation by n transmission lines of a guide which can support n modes. Two transmission lines will therefore be required to represent simultaneous propagation in the H_{01} and H_{21} modes in the circular guide. Both these lines may be regarded as being short-circuited at the position of the reflector in the circular guide, although reflection of the H_{21} mode will be somewhat imperfect due to the presence of a radial current component in this mode which the annular gap between

the reflecting disc and the guide will tend to interrupt. Since the two modes are effectively in parallel in the plane of the coupling slots, they may be represented by the transmission line system shown in Fig. 7. It is assumed that these transmission lines have

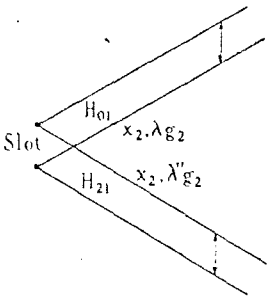

Fig. 7.—Transmission-line analogue of two-mode propagation.

phase constants equal to those of their parent modes in the circular guide, so that if the reflecting disc is placed x_2 distant from the slots in the circular waveguide, the corresponding position of each short-circuit in the equivalent transmission line system is x_2 distant from the junction.

The conditions at the junction as x_2 varies can now be considered. When x_2 has the value $\lambda_{g2}/2$, the H_{01} line will have zero input impedance, thus simultaneously short-circuiting the H_{21} line and the slot. Furthermore, no excitation of the H_{21} line occurs when the short-circuit has this particular position. The corresponding situation in terms of the prototype waveguide junction is that in which the reflecting disc is $\lambda_{g2}/2$ from the plane of the slots, when there will be no excitation of H_{21} mode in the cylindrical guide and perfect transmission in the rectangular guide. For other positions of the reflecting disc close to the correct one, a small amount of H_{21} mode is to be expected. A simple transmission-line calculation shows that the ratio of H_{21} to H_{01} excitation should be given by

$$\frac{H_{21}}{H_{01}} = k\frac{\sin \beta_2 x_2}{\sin \beta''_2 x_2} \quad . \quad . \quad . \quad . \quad . \quad (22)$$

where k is a constant depending on the effective characteristic impedances of the two lines, and $\beta_2 = 2\pi/\lambda_{g2}$ and $\beta''_2 = 2\pi/\lambda''_{g2}$ are the phase constants for the H_{01} and H_{21} modes respectively in the cylindrical guide.

Near the correct disc position ($\beta_2 x_2 \simeq \pi$) the denominator of this expression may be regarded as constant and the fractional excitation of H_{21} mode is seen to be directly proportional to the departure of x_2 from $\lambda_{g2}/2$, with a reversal of sign on passing through this position. These deductions are confirmed by the experimental results shown in Fig. 6.

It is clear that the mode-purifying wires play no great part in determining the angular distribution of field, and it was decided to remove them, relying entirely on the mode selection effect to ensure adequate mode purity.

Measurements of the angular field distribution without mode-purifying wires were made, and Fig. 8 shows the result. For a correct setting of the piston, a reasonable degree of uniformity can be achieved, as shown in the curve for a micrometer drive reading $x''_2 = 1{\cdot}7$ cm. Optimum matching and angular distribution were again found to occur at very closely similar values of x''_2. It was concluded that the mode-purifying wires were not essential, and that an adequately pure H_{01} mode could be achieved by the mode-selection effect alone.

One further point of interest emerges from the transmission-line analogue of Fig. 7, if the roles of the H_{01} and H_{21} lines are interchanged and the short-circuits are set $\lambda''_{g2}/2$ from the junction. The slot will then be short-circuited by the H_{21} line,

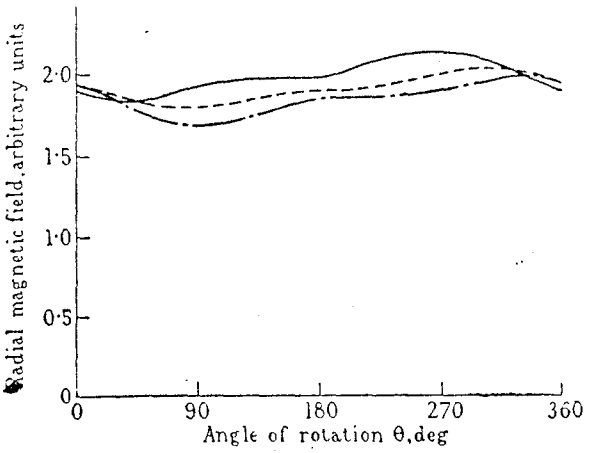

Fig. 8.—Angular field distribution in circular guide without mode-purifying wires.

$x''_2 = x_2$ — constant.
$x_2 \simeq 10$ cm.
——— $x''_2 = 1{\cdot}8$ cm.
– – – – – $x''_2 = 1{\cdot}7$ cm.
—·—·— $x''_2 = 1{\cdot}6$ cm.

and there will be no excitation of the H_{01} line. It would therefore be expected—if reflection of the H_{21} mode from the reflecting disc in the circular waveguide is nearly perfect—that if this disc is set $\lambda''_{g2}/2$ from the plane of the slots, there would be perfect matching in leg 1 of the main guide, if leg 3 is perfectly matched, and pure H_{21} mode excitation of leg 2. The results of an experiment made under these conditions is shown in Fig. 9, and

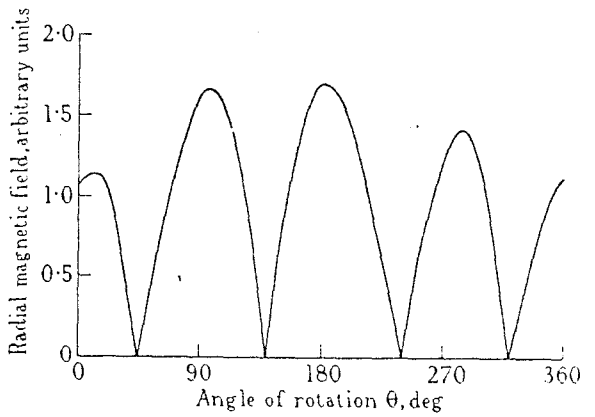

Fig. 9.—Angular field pattern for H_{21} mode operation without mode-purifying wires.

$x_2 \simeq 6{\cdot}6$ cm.
$s_1 = 0{\cdot}97$ (optimum).

although a marked odd symmetry is also present, the angular field distribution quite closely follows the theoretical $|\sin 2\phi|$ form. The standing-wave ratio in leg 1 under these conditions was 0·97, and this was the optimum value when operating in this region of values of x_2. Precise agreement of theory and experiment should not be expected, because some power undoubtedly leaks past the reflecting disc under these conditions of operation, but the results confirm the general correctness of the mode selection theory.

Summing up, it has been shown that almost pure H_{01} mode propagation is obtainable in the slot-coupled circular waveguide when the reflecting disc is placed so that a travelling wave in the main guide suffers no reflection at the junction.

(2.4) Experimental Determination of the Parameter m

The experimental method of determining m is based essentially on measurements of susceptance in the main guide as a function of the position of the reflecting disc.

Watson[12] gives the relationship between the normalized admittances Y_1 and Y_3 in the main guide and the normalized impedance Z_2 in the circular guide as

$$\frac{1}{Y_1 - Y_3} = \frac{m}{Z_2} - j\alpha$$

If leg 3 is closed by a piston adjusted so that $Y_3 = 0$ (e.g. $x_3 = \lambda_{g1}/4$), Y_1 will be equal to the admittance coupled into the main guide by the slots.

If leg 2 is closed by a reflecting disc at x_2, so that the normalized impedance Z_2 is equal to $j \tan \beta_2 x_2$ then, neglecting small losses, the normalized input admittance Y_1 will be purely susceptive, say, jB_1, and we have

$$1/B_1 = m \cot \beta_2 x_2 + \alpha \quad . \quad . \quad . \quad . \quad (23)$$

If B_1 is measured for various values of x_2 and its reciprocal is plotted in terms of $\cot \beta_2 x_2$, a straight line of slope m and intercept α should result.

The determination of B_1 can best be achieved by a method which does not involve knowledge of the absolute values of x_1 and x_3 but only increments in these quantities. Such a method is due to Feenberg,[13] and has been developed somewhat by the present author.[14]

The experimental arrangement is shown in Fig. 10(*a*). Leg 3

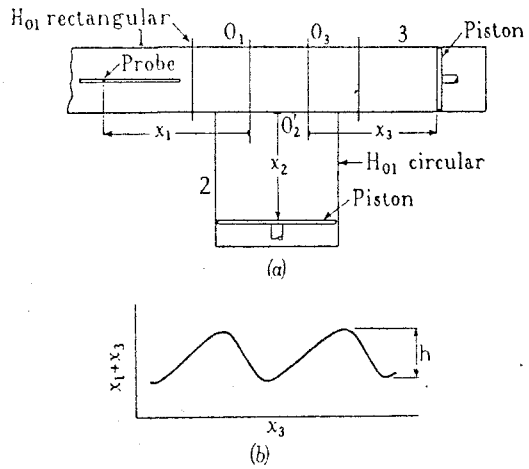

Fig. 10.—T-junction impedance measurements.
(*a*) Arrangement of guides.
(*b*) Typical nodal-separation diagram for Feenberg's method.

is closed by a movable piston at x_3 and leg 1, which includes a slotted section and moving probe to act as a standing-wave indicator, is fed from a klystron oscillator. Considerable attenuation is introduced between the klystron and the standing-wave detector, in order to avoid frequency pulling by variations in the purely reactive load during the experiments.

The experimental procedure is to set x_2 to a given length, locate a node of electric field in leg 1 at x_1 say, with the piston in leg 3 at x_3, then alter x_3, note the value of x_1 corresponding to the new position of the node in leg 1, and continue this process until sufficient points have been obtained. If $x_1 + x_3$ is plotted against x_3, the resulting curve will have the general shape indicated in Fig. 10(*b*).

The height, h, of the ripple is a measure of the discontinuity at the junction. If x_2 is chosen so that the slot-coupled section is indistinguishable from a section of uniform rectangular guide, the nodal planes in leg 1 will move along uniformly with the piston in leg 3, so that the distance between the piston and a node will not change, i.e. $x_1 + x_3$ will be constant and the ripple height will be zero.

For this value of x_2, a travelling wave in leg 1 will pass into leg 3 without reflection; this is the condition in which the T-junction is operated in the radiation-pressure application.

At any other setting there is a simple relationship between the ripple height h and the magnitude of the reflection coefficient $|\rho_1|$ which would be present in leg 1 if leg 3 were perfectly matched. This relationship is

$$|\rho_1| = \sin \frac{\beta_1 h}{2} \quad . \quad . \quad . \quad . \quad . \quad (24)$$

This result is of general application, but in the case under consideration the reflection is known to be due to the normalized susceptance B_1 introduced by the junction, and it is possible to relate this to h directly. If leg 3 is matched, its normalized admittance is purely conductive and equal to unity, and the total normalized admittance at the junction is $1 + jB_1$. The reflection coefficient for electric field is therefore

$$\rho_1 = \frac{-jB_1}{2 + jB_1}$$

whence

$$|\rho_1| = \frac{B_1}{\sqrt{(4 + B_1^2)}}$$

Solving for B_1 gives $B_1 = 2|\rho|/\sqrt{(1 - |\rho_1|^2)}$

Using eqn. (24) for $|\rho_1|$ gives

$$B_1 = 2 \tan (\beta_1 h/2)$$

Eqn. (23) can now be re-written directly in terms of the measured ripple height h thus

$$\frac{1}{2 \tan (\beta_1 h/2)} = \frac{m}{\tan \beta_2 x_2} + \alpha \quad . \quad . \quad . \quad (25)$$

When $\beta_2 x_2 = \pi$, $h = 0$, and this is the required operating position. If $x_2 = \pi/\beta_2 + l$, where l is small, $\tan \beta_2 x_2 \simeq \beta_2 l$. Under these conditions, h will be small, and $2 \tan (\beta_1 h_1/2) \simeq \beta_1 h$.

Provided that $m/\beta_2 l \gg \alpha$

$$h = \left(\frac{\beta_2}{\beta_1} \frac{1}{m}\right) l$$

or

$$h = \left(\frac{\lambda_{g1}}{\lambda_{g2}} \frac{1}{m}\right) l \quad . \quad . \quad . \quad . \quad . \quad (26)$$

If values of h determined by the method explained earlier are plotted as a function of the corresponding values of l, a straight line will result if the approximations involved in eqn. (26) are justifiable. From the slope of this, the value of $1/m$ can be found, if λ_{g1} and λ_{g2} are known. The correct matching position of the disc is not known until after the experiment, so that instead of measuring l directly, $l + l_0$ is measured from an arbitrary origin. Plotting h against $l + l_0$ gives the same slope as before, and the intercept on the $l + l_0$ axis gives the correct position of the disc relative to the arbitrary origin.

The experimental results were analysed by the method of least squares, and the regression line of h on $l + l_0$ was calculated by the standard statistical procedure.

The slope of the regression line (the regression coefficient) is $-3{\cdot}224$ with a standard deviation of $0{\cdot}080$. This gives for $1/m$ the value $5{\cdot}58$, with a standard deviation of $0{\cdot}14$, compared with the value $5{\cdot}78$ obtained theoretically from eqn. (21).

(3) EXPERIMENTAL MEASUREMENT OF POWER

Figs. 11(*a*) and 11(*b*) show the arrangement of the apparatus employed in the tests. A movable reflector in the circular-section waveguide is supported by a horizontal arm supported at its centre on a phosphor-bronze-strip suspension and balanced by a suitable counterweight at the other end. The small force exerted by radiation on the reflector produces a small rotation of the moving system about the axis of the suspension, and this rotation is measured by means of a lamp and scale associated with a small concave mirror attached to the torsion arm. If the specific couple of the suspension is known, the force can be calculated, and the results given in Section 2.4 enable the power to be found.

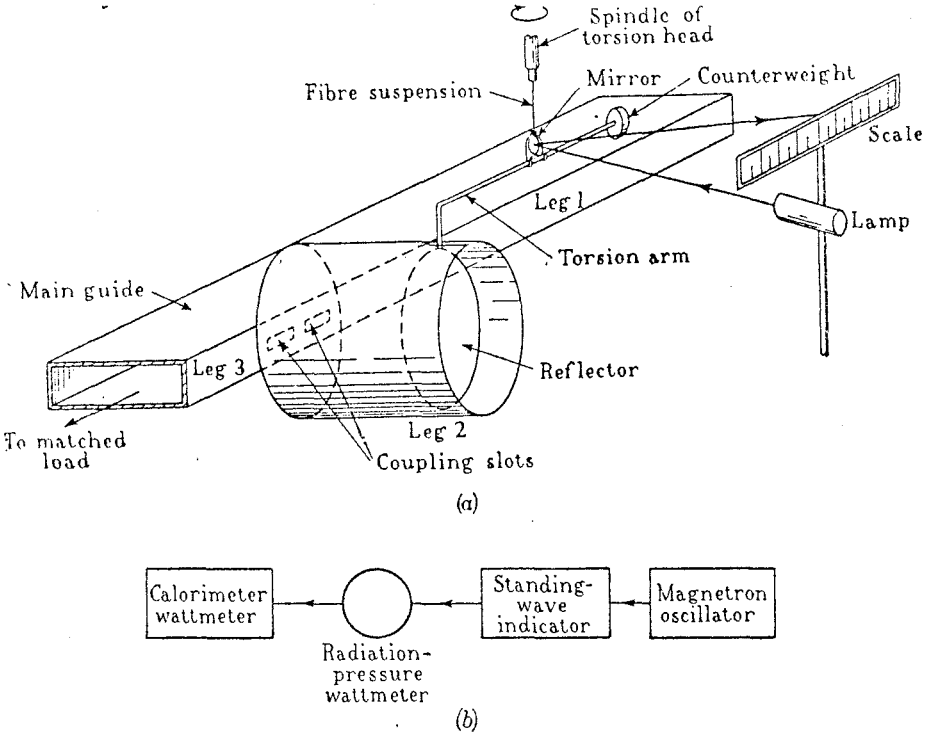

Fig. 11.—Apparatus for power measurement by radiation pressure.
(*a*) Arrangement for direct measurements.
(*b*) Schematic of apparatus for comparison measurements.

(3.1) Preliminary Experiments

(3.1.1) The Reflector.

In the first experiments the reflector was a disc of aluminium foil mounted on an aluminium-wire ring to give it the necessary rigidity. The torsion arm was completely enclosed, the coupling slots were covered with Styrafoil 0·0005 in thick and a circular glass plate covered the open end of the circular waveguide, so that the apparatus was shielded from external draughts.

However, it rapidly became apparent that the mechanical behaviour of the torsion balance was unsatisfactory. In the first place, the movement was found to be very heavily overdamped. Secondly, it was impossible to obtain a stable zero setting, even on a relatively short-term basis of a minute or so. This continual wandering of the movement was due to convection currents set up by small and changing temperature gradients within the enclosed apparatus.

The remedy adopted was to reduce the air resistance of the reflector so that the convection currents would have no appreciable effect and damping would be reduced.

The method makes use of the fact that the electric vector in the circular guide is wholly circumferential. A system of concentric wire rings such as that shown in Fig. 12 may be expected to act as an almost perfect reflector of the electromagnetic waves, but at the same time it will have a small effective cross-section to air currents. The electromagnetic theory of such a system of rings has not yet been worked out, so far as the author is aware, and the only relevant theory is the calculation of the reflecting properties of a system of parallel straight wires with a plane wave obliquely incident made by MacFarlane.[15] It is reasonable to suppose that this calculation will give qualitatively correct predictions of the effect of altering wire diameter and wire

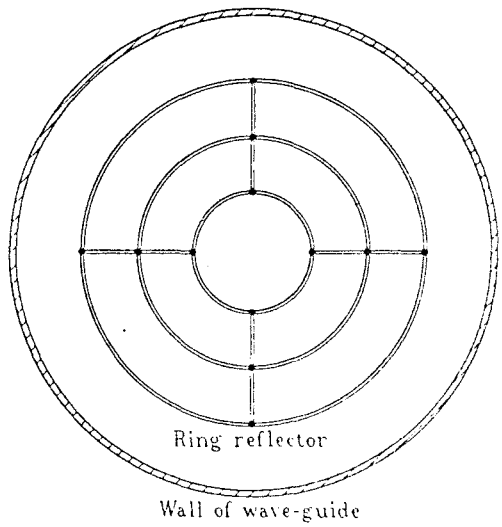

Fig. 12.—3-ring reflector.

spacing, and might even yield a rough value for the normalized reactance of the ring system. Qualitatively, if the wires are close together in comparison with the wavelength, the reactance will be small. Increasing the wire diameter reduces the reactance, but the effect is logarithmic and therefore not marked. One ring reflector employed used three 22 S.W.G. tinned copper-wire rings of radii 1·5, 3·0, and 4·5 cm. MacFarlane's theory shows that a reflector of parallel 22 S.W.G. wires at 1·5-cm spacing has a normalized reactance of 0·144 relative to the normalized wave impedance of a plane wave obliquely incident at an angle $\theta = \arccos \lambda/\lambda_{c2}$ (corresponding to the half-angle of the cone of elementary plane waves represented by the Sommerfeld integral[16] formula for the Bessel functions). Only 4% of the incident power would leak past the reflector, and this figure is a guide to the order of magnitude of the loss to be expected in the waveguide case. For other reflector systems with more rings the leakage is considerably reduced. The force acting on the ring system may be deduced theoretically if the reflection is almost perfect, in the following way.

Imagine an ideal ring reflector (or any perfect reflector) and a disc reflector separated by about $\lambda_{c2}/2$ in a length of loss-free circular waveguide, the exact separation d being chosen in such a way that resonance of the H_{01} mode takes place. Since it has been postulated that there is neither power leakage nor conductor losses, the resonance, once established, will persist indefinitely. If the rings and the disc are slowly moved a distance x along the guide in such a way that their separation is unchanged, the work done is $(F - F')x$ if the force due to radiation on the disc is F and that on the rings is F'. This must equal the work done if the guide is moved a distance x in the opposite direction with the rings remaining stationary, since the relative movement is the same in both cases. However, the force exerted by an electromagnetic wave on a perfectly conducting metal surface is wholly normal to the surface, since $\mathscr{E}$ is normal and H tangential, and so the work done in moving the guide parallel to its axis through a distance x is zero. It follows that $F = F'$, and therefore the force on any perfectly reflecting obstacle is the same as that on the disc. This is true even though there may be considerable phase change on reflection, provided only that there is no amplitude change.

In order to avoid any loss of power by leakage past the rings, the circular guide was continued for one-quarter of a guide wavelength beyond the ring reflector, and closed by a metal plate. Experiments to find $1/m$ for a ring-reflector system were then made with the quarter-wave guard section in position. Determination of $1/m$ for a reflector having five concentric rings gave a value 5·56 with a standard deviation of 0·055, as compared with 5·58 with a standard deviation of 0·14 for a solid disc. There is therefore no significant electrical difference between the ring reflector and the solid disc when the latter is correctly aligned in the guide. However, it is obviously difficult to ensure correct alignment when the reflector is suspended from a delicate torsion balance, and experiments were therefore made to determine $1/m$ with deliberate misalignment; the results are shown in Table 2.

If square-law variation of $1/m$ with offset or tilt is assumed, $1/m$ will not be significantly affected if the offset is not greater than 3 mm and the tilt not greater than 1°. These requirements are easily met.

(3.1.2) Effect of Load on Specific Couple of Suspension.

The suspension used in the torsion balance was a phosphor-bronze strip of the type used in galvanometers. The specific couple of a given suspension was determined by timing its period of oscillation with a known moment of inertia. Since several different movements of differing weight were used in the experiments, it was felt to be desirable to check the periodic time under various conditions of load. The differences found were not significant, if possible experimental errors are taken into account, and it is reasonable to assume that no serious error will be made in assuming that the specific couple is the same—about 6·4 dyne-cm/radian—for all the movements used, all of which have weights in the range 10–15 gram.

Table 2

EFFECT OF ASYMMETRY IN REFLECTOR POSITION

Arrangement	Value of $1/m$	Standard deviation
Symmetrical; plane perpendicular axis ..	5·56	0·055
Displaced 3·0 mm vertically; plane perpendicular axis	5·47	0·052
Displaced 3·2 mm horizontally; plane perpendicular axis	5·59	0·035
Symmetrical; tilted 2·5° about vertical axis	5·66	0·059
Symmetrical; tilted 2·7° about horizontal axis	5·37	0·028

(3.1.3) The Torsion Balance.

For speed and ease of reading, it was desirable that the torsion balance should have a dead-beat response, and to achieve this the reduction in air resistance brought about by the use of a ring reflector was offset by the addition of a dashpot damper containing a silicone fluid. It was found possible to arrange the damping to give about 1% overshoot. Typical response curves are shown in Figs. 13(*a*) and 13(*b*).

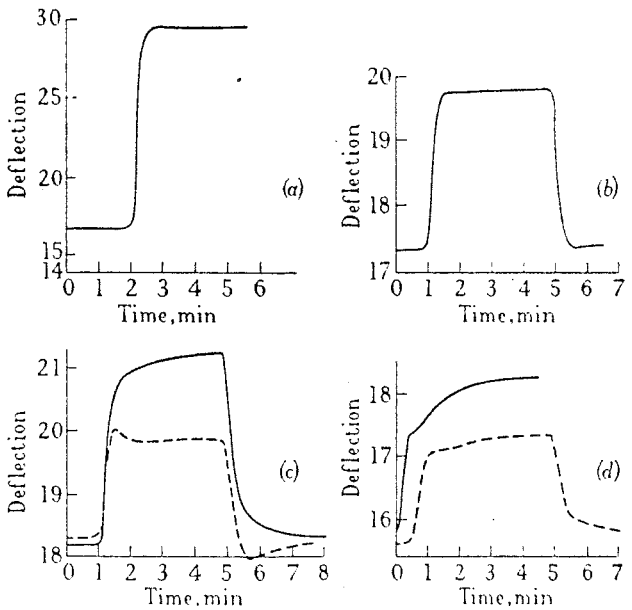

Fig. 13.—Deflection/time curves for several reflectors under different conditions.

(*a*) Torsion head turned suddenly; 0·8% overshoot. 3 copper rings of 20 S.W.G.
(*b*) Magnetic field applied suddenly, then withdrawn suddenly. 3 copper rings of 20 S.W.G.
(*c*) Oscillator switched on for 5 min. 3 copper rings of 20 S.W.G.
———— Power ≃ 25 watts.
– – – – – Power ≃ 12·8 watts.
(*d*) Oscillator switched on for 5 min.
———— Power ≃ 40 watts. 5 aluminium rings of 18 S.W.G.
– – – – – Power ≃ 36 watts. 3 copper rings of 20 S.W.G.

(3.1.4) Drift.

In preliminary tests of the complete apparatus it was found that, on switching on the microwave power, the deflection rose comparatively rapidly to a value corresponding approximately

to the force due to radiation pressure and subsequently drifted to a different value (usually greater) in the course of about 5 min. Some examples are shown in Figs. 13(*c*) and 13(*d*). The effect was thought to be due to convection currents in the cavity set up by the heat dissipated in the reflector under operating conditions. A rough estimate of the thermal time-constant of the ring system supported this view.

The hypothesis of convection currents was tested for a particular ring system by calculating the r.f. power dissipated in it—which proved to be 0·05 watt with 30 watts in the main guide—and then introducing a comparable amount of heating by a small carbon resistor mounted inside the cavity near the rings and heated by 50-c/s supply. (The microwave power was switched off during this test.)

The deflection of the ring system in this test was found to agree in magnitude and time of build-up with the drift found under microwave operating conditions. Further evidence was provided by the discovery that the effect of the convection currents could be modified by paper wind-deflectors inside the cavity.

Various ring systems were tried in the hope that a design giving very little drift would be found, but without much success. Wide variations in the form of the drift were found, and these were apparently largely caused by quite minor changes in the geometry of the system.

(3.2) Detailed Comparison of Calorimetric and Radiation-Pressure Power Measurement

(3.2.1) General.

In the experiments about to be described, the general arrangement of the apparatus was as shown in the schematic diagram of Fig. 11(*b*). The object was to make simultaneous measurements of power with the radiation-pressure apparatus and a calorimeter wattmeter of the type described by Turner.[17] In order to avoid errors in the radiation-pressure measurement, it was necessary to take special care over the matching of the water load, and a standing-wave ratio between 0·990 and 0·997 in the wavelength range 9·05–9·15 cm was achieved. Heat losses from the water load and the balancing calorimeter were adjusted so that no systematic dependence of indicated power on water-flow rate from 3 to 9 cm³/sec could be detected.

In order to avoid constant repetition of the rather laborious calorimeter measurement, the magnetron oscillator was calibrated for power output against voltage on the h.v. transformer primary when working into a matched load. The calibration was checked from time to time.

(3.2.2) Direct Method.

Some detailed comparisons of the radiation-pressure and calorimeter wattmeters will now be considered: First, observations made with the movement almost critically damped, and giving deflection/time curves similar to those of Fig. 13 will be discussed.

In Table 3, a set of results obtained from the radiation-pressure wattmeter is shown, a 20-S.W.G. 3-ring copper reflector being used. Mechanical tests [as shown in Fig. 13(*a*)] showed that the movement took about 45 sec to reach the maximum of its 0·8% overshoot, but that after 30 sec the deflection was only 1·8% less than the final deflection and was changing very slowly. In order to minimize errors due to convection-current effects, the deflection after 30 sec was noted, and the final deflection computed from it by multiplying by 1·018. Deflections were measured both for switching on and switching off the transmitter, and on the whole, better agreement was obtained in the latter case. It might be thought that this is due to a change in the power of the oscillator in the first few minutes after switching on, but a neon-tube standing-wave detector which acts as a measure of relative power shows that the transmitter develops its full output almost immediately after switching on.

Table 3

COMPARISON OF POWER MEASUREMENTS WITH 3-RING COPPER REFLECTOR

Power measured	
By calorimetric method	By radiation-pressure method
watts	watts
15	13·0
16	15·5
21	17·5
27	24·5
31	28·0
39	37·5

Results obtained with the 5-ring aluminium system and shown in Table 4 are rather more satisfactory, presumably because of the very pronounced step in the deflection/time curves which makes the determination of the true radiation-pressure deflection more reliable.

Table 4

COMPARISON OF POWER MEASUREMENTS WITH 5-RING ALUMINIUM REFLECTOR

Power measured	
By calorimetric method	By radiation-power method
watts	watts
46·5	46·0
40·5	39·0
31·5	32·0
26·0	24·5
17·0	15·5
11·0	10·0

(3.2.3) Semi-Ballistic Method.

Nichols and Hull employed a semi-ballistic method to avoid residual air-current and radiometer effects, and it was thought worth while to try this method with the present apparatus.

If the movement is completely free from damping and has a periodic time T, and if the oscillator is switched on for a time $T/4$ with the movement initially at rest, the first maximum deflection observed after switching off is $\theta_0\sqrt{2}$, where θ_0 is the final deflection which the oscillator would produce under steady-state conditions. Thus, observing this maximum would suffice to determine θ_0, and hence the power.

If the movement is damped, and satisfies an equation of the form

$$Id^2\theta/dt^2 + \gamma d\theta/dt + c\theta = 0$$

its free oscillations will decay exponentially. Let r_2 be the ratio of amplitudes in successive periods. If the oscillator is switched on for one-quarter of the periodic time, the first maximum deflection observed will be

$$\theta_0\sqrt{2}\left(1 - \tfrac{1}{2}\log_e\frac{1}{r_2}\right) \quad . \quad . \quad . \quad . \quad . \quad (27)$$

to a close approximation for small damping, i.e. when γ is small. Thus, if r_2 is known, θ_0 can again be determined from an observation of the semi-ballistic throw.

The foregoing theory is applicable only when γ in the differential equation of motion is constant. A sufficient criterion is the constancy of r_2 computed from successive maxima and minima when the movement is allowed to swing freely. The results of such a test are recorded in Table 5, which relates to the 3-ring 20 S.W.G. copper reflector.

Table 5

CONSTANCY OF r_2 WITH VARIATION OF OSCILLATION AMPLITUDE

Maxima	Minima	Difference between successive maxima and minima, A_n	Value of $r_2 = \frac{A_n}{A_{n-1}}$
30·56			
	21·35	9·21	
29·50		8·15	0·885
	22·30	7·20	0·884
28·68		6·38	0·885
	23·05	5·53	0·867
28·00		4·95	0·895
	23·60	4·40	0·888
27·50		3·90	0·885
	23·98	3·52	0·901

It will be seen that r_2 is constant to a high degree of accuracy, and the mean value obtained by averaging the final column is 0·886.

Substitution in eqn. (27) shows that the maximum deflection obtained after switching the oscillator on for one quarter-period is $1{\cdot}33\theta_0$. The periodic time of the movement is 50·7 sec, so that the quarter-period is only 12·7 sec. In all previous tests, the oscillator was in operation for at least 30 sec before a deflection was recorded, and so the present ballistic technique represents a considerable improvement in reducing the amount of heat supplied to the reflector.

A set of results obtained by this method is given in Table 6. The discrepancy between the radiation-pressure measurement and the calibration curve is never greater than 2 watts.

Table 6

COMPARISON OF POWER MEASUREMENTS USING SEMI-BALLISTIC METHODS

Power measured	
By calorimetric method	By radiation-pressure method
watts	watts
11·5	10
15	13·5
24	24
32	30
36·5	36·5
40	41

(3.4) Discussion of Results

It appears from the results of the preceding Sections that the calorimeter wattmeter gives a power figure somewhat greater than that obtained from the radiation-pressure apparatus in nearly all cases.

There is no significant variation in this difference, expressed in watts, with the power being measured. Averaged over all the experimental results obtained, the discrepancy is $1{\cdot}3 \pm 0{\cdot}7$ watts (the limits are taken as $\pm$ 3 times the standard deviation), or $+0{\cdot}6$ to $+2{\cdot}0$ watts. It is necessary to inquire whether this discrepancy is significantly greater than can be accounted for in uncertainties in the constants of the two wattmeters. For the radiation-pressure wattmeter, the only appreciable systematic errors arise from the determinations of $1/m$ and the specific couple of the suspension. At an average power level of 25 watts, these errors combine to give a possible error of $\pm 0{\cdot}6$ watt (thrice the standard deviation). There is a further possible error due to residual convection current errors, but it is impossible to give a reliable estimate of this error from the data available.

Probably the only significant systematic error in the calorimeter wattmeter is incurred in the measurement of the current flowing in the heater of the balancing calorimeter. The ammeter used is classified as B.S.I. Grade I, and should be accurate to within $\pm 1\%$. This corresponds to a $\pm 2\%$ error in power, or $\pm 0{\cdot}5$ watt at 25 watts. If the B.S.I. classification is taken as roughly corresponding to thrice the standard deviation this can be combined with the same overall figure of the radiation-pressure apparatus to estimate the limits of the systematic discrepancy as $\pm 0{\cdot}8$ watt. Comparison of this figure with the observed discrepancy of 0·6–2·0 watts shows that there is no significant difference between the calorimeter and wattmeter results.

(4) CONCLUSIONS

The practical possibility of absolute measurement of microwave power by radiation pressure may reasonably be regarded as established by the results described in the paper.

Two particular features of the radiation-pressure method should be noted. First, it is absolute, in the sense that it depends only on measurements of mass, length, and time. Secondly, it is particularly suitable for comparison or calibration purposes, because it does not absorb any power, and can be used simultaneously with an absorbing wattmeter.

The usefulness of the method will, of course, depend largely on the extent to which its accuracy can be improved. Further experiments are in progress with a modified apparatus, and it is hoped that these experiments will lead to the desired increase in accuracy.

(5) ACKNOWLEDGMENTS

The author wishes to thank Prof. R. O. Kapp for the use of the facilities of his laboratories and for his interest in the work, Prof. H. M. Barlow for his constant encouragement and for many valuable discussions, and Mr. H. G. Effemey for many useful suggestions and much practical assistance.

Thanks are also due to Messrs. F. W. Rason and W. Woodward for their skilful construction of most of the apparatus.

(6) REFERENCES

(1) MAXWELL, J. C.: "A Treatise on Electricity and Magnetism," 1st edition (Oxford, University Press, 1873), p. 391.

(2) BARTOLI, A.: "Sopra i movimenti prodotti dalla luce e dal calore" (Le Mounier, Florence, 1876).

(3) LEBEDEW, P.: "Rapports présentés au Congres International de Physique" (Paris, 1900), **2**, p. 133.

(4) NICHOLS, E. F., and HULL, G. F.: "The Pressure due to Radiation," *Proceedings of the American Academy of Arts and Sciences*, 1903, **38**, p. 559.

(5) HUSSON, S.: "Action mécanique exercée sur un conducteur par les ondes electromagnétiques," *Comptes Rendus*, 1930, **191**, p. 33.

(6) FRITZ, K.: "Die Messung der ponderomotorischen Strahlungskraft auf Resonatoren im elektromagnetischen Feld," *Annalen der Physik*, 1931, **11**, p. 987.

(7) CARRARA, N., and LOMBARDINI, P.: "Radiation Pressure of Centimetre Waves," *Nature*, 1949, **163**, p. 171.
(8) CULLEN, A. L.: "Absolute Power Measurement at Microwave Frequencies," *ibid.*, p. 413.
(9) CULLEN, A. L.: "Absolute Measurement of Microwave Power by Radiation Pressure," *ibid.*, 1950, **165**, p. 726.
(10) HUXLEY, L. G. H.: "Wave Guides" (Cambridge University Press), p. 170.
(11) ALLANSON, J. T., COOPER, R., and COWLING, T. G.: "The Theory and Experimental Behaviour of Right-Angled Junctions in Rectangular Section Wave Guides," *Journal I.E.E.*, 1946, **93**, Part III, p. 177.
(12) WATSON, W. H.: "Wave Guide Transmission and Antenna Systems" (University Press, Oxford), p. 115.
(13) FEENBERG, E.: "Relation Between Nodal Positions and Standing Wave Ratio in a Complex Transmission System," *Journal of Applied Physics*, 1946, **17**, p. 530.
(14) BARLOW, H. M., and CULLEN, A. L.: "Micro-wave Measurements" (Constable, London, 1951), p. 194.
(15) MACFARLANE, G. G.: "Surface Impedance of an Infinite Parallel-wire Grid at Oblique Angles of Incidence," *Journal I.E.E.*, 1945, **93**, Part IIIA, p. 1523.
(16) LAMONT, H. R. L.: "Wave Guides" (Methuen Monographs on Physical Subjects, 1942), p. 67.
(17) TURNER, L. B.: "Balanced Calorimeters for 3 000 and 10 000 Mc/s with Tapered Water Loads for H_{01} Rectangular Pipes," *Journal I.E.E.*, 1945, **93**, Part IIIA, p. 1467.